energies

MDPI

Article

Research on Energy Management Strategy of Fuel Cell Electric Tractor Based on Multi-Algorithm Fusion and Optimization

Hongtu Yang [1,2], Yan Sun [1,*], Changgao Xia [1,*] and Hongdang Zhang [2]

[1] School of Automotive and Traffic Engineering, Jiangsu University, Zhenjiang 212013, China
[2] Department of Vehicle Engineering, Changzhou Vocational Institute of Mechatronic Technology, Changzhou 213164, China
* Correspondence: 2111904003@stmail.ujs.edu.cn (Y.S.); xiacg@ujs.edu.cn (C.X.)

Abstract: To solve the serious pollution problems of traditional fuel tractors and the short continuous operation time of pure electric tractors, a hybrid tractor with fuel cell as the primary power source and battery as the auxiliary power source is proposed. A novel energy management strategy was also designed, which integrates thermostat control strategy, power following strategy, and fuzzy logic control. The energy management strategy utilizes the advantages of different algorithms and realizes the rational distribution of fuel cell and battery output power. The system economy and fuel cell durability are improved by the tabu search algorithm. The simulation results show that the proposed energy management strategy can work well in different SOC states and reduce the fuel cell's power fluctuations. The tractor is equipped with 960 g of hydrogen, the initial state of charge (SOC) is 90%, and it can operate continuously for 2.65 h.

Keywords: fuel cell; energy management; power following strategy; fuzzy logic control strategy; tabu search algorithm

check for updates

Citation: Yang, H.; Sun, Y.; Xia, C.; Zhang, H. Research on Energy Management Strategy of Fuel Cell Electric Tractor Based on Multi-Algorithm Fusion and Optimization. *Energies* **2022**, *15*, 6389. https://doi.org/10.3390/en15176389

Academic Editors: Eric Cheng and Junfeng Liu

Received: 16 July 2022
Accepted: 29 August 2022
Published: 1 September 2022

Publisher's Note: MDPI stays neutral with regard to jurisdictional claims in published maps and institutional affiliations.

Copyright: © 2022 by the authors. Licensee MDPI, Basel, Switzerland. This article is an open access article distributed under the terms and conditions of the Creative Commons Attribution (CC BY) license (https://creativecommons.org/licenses/by/4.0/).

1. Introduction

Along with the advancement of science and technology, traditional agriculture is also developing in the direction of electricity, intelligence, and greening [1–3]. As the primary tool of agricultural production, tractors can replace laborious farming operations and play a vital role in the development of agriculture [4]. Traditional tractors are mainly equipped with diesel engines as the power source. Diesel engines have high reliability, long service life, and mature technology, but there are also problems of exhaust emission and noise, and diesel engines are not suitable for operation in greenhouses [5]. Different from traditional tractors, electric tractors have the advantages of low working noise, simple structure, no pollutant emission, and high energy utilization rate, which are in line with the development trend of electricity and greening [6].

The operation time of pure electric tractors on the market mainly depends on the capacity of the battery [7]. The operating time of pure electric tractor, which uses the battery as the single power source, is about 4 to 5 h. However, the charging time of pure electric tractor is about 5 to 6 h, and the longer charging time significantly limits the continuous operating time of pure electric tractors. To solve the problem of short working times in pure electric tractors, hybrid tractors were developed [8]. The hybrid tractors use diesel engines as range extenders and batteries as the primary power source. These new tractors can keep the battery state of charge (SOC) at an appropriate level through energy management strategy (EMS), solving the problem of slow battery charging, and the tractor can work all day due to the fast diesel fueling rate. However, the hybrid tractor does not solve the problem of pollutant emission. Although EMS can make the diesel engine work in the high-efficiency area all the time, and the pollutant emission is significantly reduced, this kind of tractor still cannot be used in the greenhouse.

In recent years, fuel cells have attracted more and more attention due to their high-power generation efficiency, non-polluting, fast fueling, and low noise [9]. However, problems such as high price, short service life, and inadequate hydrogenation facilities have restricted the further promotion of fuel cells. At the same time, fuel cells have poor output characteristics and cannot discharge as quickly as batteries. Ultracapacitors, batteries, and other combinations are used to solve the problems existing in the use of fuel cells. Therefore, the EMS of multi-power sources has become a key issue affecting the power and economy of electric tractors.

Based on literature research, the EMSs are mainly divided into three categories [10,11]: rule-based strategies, optimization-based strategies, and artificial-intelligence-based strategies.

The main idea of the rule-based energy management strategy is that the input signal determines its output signal according to pre-designed rules. The advantages of this type of control strategy are that it can be controlled online in real time, and the algorithm is easy to implement. Rule-based strategies can be divided into two categories according to the expression of rules: deterministic rules and fuzzy rules [12,13]. The former mainly includes control strategies such as logic threshold, thermostat control strategy, and power-following strategy. These control strategy rules determine the threshold in advance according to experience, with strong real-time performance and low adaptability. Geng [14] proposed an on–off power following control strategy. It can be seen that the hydrogen consumption of the power following control strategy using fuzzy algorithm is 6.9% lower than that of the on–off power following control strategy, while the total mileage is 7.1% higher. The fuzzy rules mainly refer to the control strategy of fuzzy logic strategy [15]. Compared with the deterministic rules, the exact threshold value is not required, but the structure of "if, then..." is used to express the rules in the fuzzy language. Jin [16] distributes power based on the operation mode of the vehicle and the real-time voltage of the ultracapacitor. Through simulation, the fuzzy logic EMS can reduce the battery degradation by 17%. Fuzzy logic strategy has strong robustness but easily falls into local optimum. It should be pointed out that expert experience is particularly important for the design of fuzzy rules. Some scholars adopt optimization algorithms to improve the performance of fuzzy controllers. Relevant parameters such as membership function or weight coefficients of fuzzy rules are optimized to enhance their ability of global control. Although rule-based EMS has the disadvantage of easily falling into local optimum, its advantages of high real-time, good compatibility, and simplicity make it widely used in practice.

The EMSs based on optimization can be divided into global optimization and real-time optimization [17–19]. Global optimization algorithms mainly include Dynamic Programming (DP) [20] and Pontryagin's minimum principle (PMP) [21]. The DP algorithm is often used as the optimal reference benchmark for strategic evaluation [22]. In recent years, swarm intelligence algorithms such as Genetic Algorithm (GA) [23], Particle Swarm Algorithm (PSO) [24], and Ant Colony Algorithm (ACO) [25] have been combined to optimize the parameters of control strategy and obtain the global optimal control effect. Although the global optimization algorithm can obtain the best result, it needs to be optimized under the condition of known operating conditions and has a large number of calculations, so it is not suitable for real applications. Instantaneous optimization algorithm mainly includes equivalent consumption minimization strategy (ECMS) [26] and model prediction control (MPC) algorithm [27]. ECMS converts the energy consumed by operation into fuel consumption of the internal combustion engine (ICE), but the equivalent factor has a significant influence on the effect of the algorithm. Zheng [28] found that the fuel-saving potential of ECMS is around 4% relative to the rule-based strategy, but it may lead to frequent fluctuations in fuel cell output power, which accelerated the degradation of fuel cells. Strategy based on MPC algorithm predicts the operation state for a limited time according to historical information and current collected information. The algorithm has the advantages of feedback correction and high robustness. However, the MPC has the disadvantages of too many constraints and too much computation.

Along with the development of intelligent algorithms, some achievements have been made in the research of intelligence-based EMSs. Intelligence-based algorithms can be divided into two main categories: machine learning and reinforcement learning [29,30]. Machine learning is often combined with other algorithms to improve the accuracy and robustness of control strategies. The control strategy based on reinforcement learning is developed from Q-learning. The main advantage of reinforcement learning is that it does not need model and tedious coefficient identification work, reinforcement learning has strong robustness, and it can realize real-time control.

The tractor generally operates at a low speed and has little braking energy recovery efficiency. The operator will configure the tractor with different tools according to the operating conditions, such as rotary tillers, ploughs, etc. The load of tractors varies greatly under operating conditions such as driving, full-load transportation, rotary tillage, and ploughing. Scholars pay little attention to the issue of the dynamic loading rate of fuel cells. Taking the dynamic loading rate of fuel cells as a constraint condition of EMS will inevitably have a significant impact on the EMS of automobiles, but it has less impact on the EMS of electric tractors.

Although the current EMS can reduce the energy consumption and improve the service life of fuel cells, the input and output characteristics of fuel cells are rarely considered. When the demand current suddenly increases, the response of the fuel cells is slow. If the constructed EMS is followed, it will cause a significant deviation between the demand current and the actual current, which will affect the vehicle's power performance and economy.

To solve the problem of short continuous operation time of pure electric tractors, an electric tractor with a fuel cell as the primary energy source is put forward in this paper. A new EMS that combines rule-based and optimization-based strategies has been developed. The proposed EMS not only solves the problem of energy distribution but also improves the economy of the system by utilizing the advantages of several algorithms. The proposed EMS has strong practicability and can be well applied to fuel-cell electric tractors.

2. Fuel Cell Tractor Model

2.1. Tractor Model

The tractor developed is a small electric tractor driven by a motor. It mainly works in the greenhouse. The tractor can provide a maximum power of 15 kW. The tractor can meet different operating requirements by adjusting the suspension device. Ploughing operation has the highest traction compared to rotary tillage and transportation. An analysis of the tractor's longitudinal forces during ploughing is shown in Figure 1. The electric tractor speed is low, and the influence of air resistance is negligible. The driving force of electric tractor under ploughing conditions is shown in Equations (1) and (2) [31].

$$F_t = F_f + F_i + F_j + F_{plg} \tag{1}$$

$$P_{req} = \frac{F_t \cdot V}{1000\eta_{mec}} + P_{sl} \tag{2}$$

where F_t is the traction of the tractor, F_f is the rolling resistance, F_i is the slope resistance, F_j is the acceleration resistance, F_{plg} is the ploughing traction resistance, P_{req} is the tractor power demand, V is the tractor operating speed, η_{mec} is the mechanical transmission efficiency, and P_{sl} is the slip loss power.

Due to the complex and changeable soil conditions, the ploughing resistance of the tractor is also complex. Currently, there is no ploughing cycle similar to the driving cycle of a vehicle, and the ploughing model is generally described by empirical formulas. In this paper, the commonly used empirical formula is selected to illustrate the ploughing resistance, as shown in Equation (3) [32].

$$F_{plg} = z * b * h * k \tag{3}$$

where z is the number of ploughshares, b is the width of a single ploughshare, h is the ploughing depth, and k is the soil specific resistance. The specific resistance of soil is shown in Table 1.

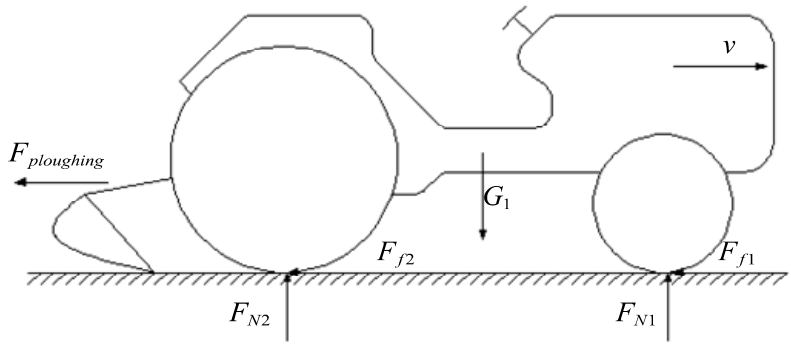

Figure 1. Force analysis of electric tractor under ploughing condition.

Table 1. Specific resistance of soil.

Type	k (N × cm^2)
sand	2~4
sandy loam	3~5
loam	4~6
clay loam	6~8
clay	8~10

The whole vehicle structure of the fuel cell tractor is shown in Figure 2. When the tractor is rotating, the PTO (power take-off) shaft will transmit power to the rotary cultivator. When the tractor is ploughing or carrying heavy loads, the PTO shaft will not transmit power, and the PTO motor is turned off. The fuel cell is connected in series with the DC/DC and then connected in parallel with the battery. The DC/DC output voltage is consistent with the battery. The vehicle parameters are shown in Table 2.

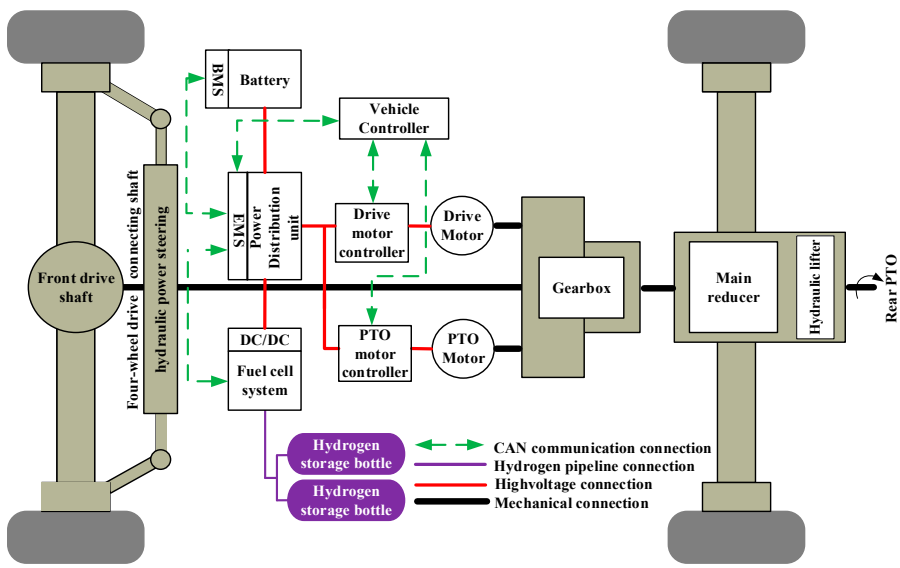

Figure 2. Architecture of fuel cell electric tractor.

Table 2. Parameters of tractor and components.

Parameters	Value
Curb weight/kg	1800
Fuel cell rated power/kW	9
Fuel cell peak power/kW	12
Number of parallel connections of FC system	3
Hydrogen weight/g	960
Drive motor power/kW	7.5
PTO motor power/kW	7.5
Motor maximum torque/Nm	125
Highest efficiency of the motor/%	88
Battery capacity/Ah	50
Battery voltage/V	130
Number of battery stacks in parallel/series	3/37

2.2. Fuel Cell Model

In this paper, a commercial fuel cell with a rated power of 9 kW is selected and matched with a hydrogen tank of 2 × 20 L and 35 MPa. The hydrogen tank can store 960 g of hydrogen. The maximum power change rate of the fuel cell can reach 300 W/s. To see the impact of diverse fuel cell efficiency on different power outputs in the EMS problem, a second-order equation is fitted to the efficiency diagram. The efficiency and voltage of the fuel cell system are obtained through the bench test, which is shown in Figure 3. The efficiency of the fuel cell is shown in Equation (4). In this paper, the fuel cell has been working in the high-efficiency region. Therefore, the effects of load change cycle and start/stop cycles on fuel cell performance degradation are mainly considered [33,34]. The fuel cell performance degradation model is shown in Equation (5).

$$\eta_{fc} = a_1 {P_{fc}}^2 + a_2 P_{fc} + a_3 \tag{4}$$

$$\begin{cases} D_{fc} = D_{change} + D_{on-off} \\ D_{change} = 5.93 \times 10^{-7} \times \sum \dfrac{\left| P_{fc}(n) - P_{fc}(n-1) \right|}{P_{high} - P_{low}} \\ D_{on-off} = 1.96 \times 10^{-5} \times \sum d_{on-off}(n) \\ d_{on-off}(n) = 1, \quad signal_{fc}(n-1) \neq signal_{fc}(n) \\ d_{on-off}(n) = 0, \quad signal_{fc}(n-1) = signal_{fc}(n) \end{cases} \tag{5}$$

where η_{fc} is the fuel cell system efficiency, P_{fc} is the fuel cell system output power, and a_1, a_2, a_3 are the coefficients. D_{fc} is the fuel cell total degradation percentage, D_{change} is the degradation caused by the load change cycles, and $D_{on\text{-}off}$ is the degradation caused by the start/stop cycles. P_{high} is the high-power threshold, P_{low} is the low-power threshold of the fuel cell under idling conditions, and $signal_{fc}(n)$ and $signal_{fc}(n-1)$ denote the FCs start signal of the nth step and $(n-1)$th step, respectively.

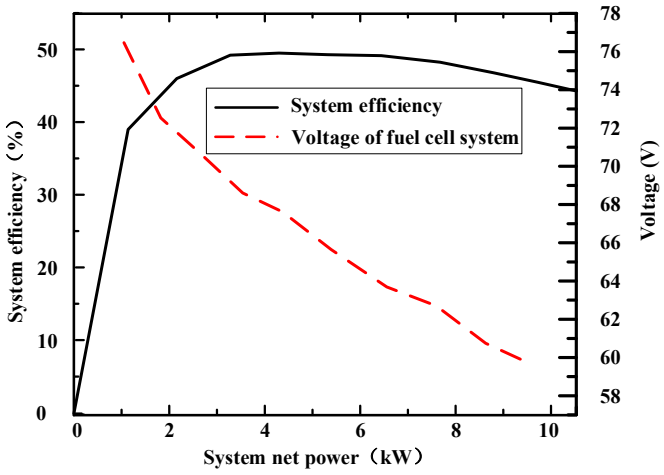

Figure 3. Fuel cell system efficiency and voltage.

2.3. Battery Model

In this paper, a lithium iron phosphate battery is selected as the auxiliary power source for the tractor. The main function of the battery is to reduce the power fluctuation of the fuel cell, absorb the output power of the fuel cell, and reduce the number of start–stop cycles of the fuel cell. *SOC* is the key parameter of the battery, which is defined in Equation (6). The relationship between battery current, voltage, and power is shown in Equation (7).

$$SOC(t) = SOC_{max} - \int_0^t \frac{I_{bat}dt}{Q_{max}} \tag{6}$$

$$I_{bat} = \frac{V_{ov} - \sqrt{V_{ov}{}^2 - 4R_{bat}P_{bat}}}{2R_{bat}} \tag{7}$$

where $SOC(t)$ is the battery state of charge, SOC_{max} is the maximum SOC, I_{bat} is the output current, Q_{max} is the capacity, V_{ov} is the open-circuit voltage, R_{bat} is the internal resistance, and P_{bat} is the output power.

3. EMS Design

Since the fuel cell is the primary power source and the battery is the auxiliary power source, the maintenance of the battery SOC is essential. Secondly, the fluctuation of the fuel cell output power should be reduced as much as possible while maintaining SOC within a reasonable range. Finally, the change rate of fuel cell output power should be kept within its dynamic output characteristic range.

3.1. SOC Maintenance Based on TCS

The thermostat control strategy (TCS) is widely used in industrial control, especially in temperature control. Similar to temperature control, the SOC of the battery is mainly stabilized between 40 and 80%. The TCS can ensure that the fuel cell always operates in the optimal area and reduce hydrogen consumption. The battery is constantly being charged and discharged, reducing its lifespan. This control strategy is disadvantageous to the battery but beneficial to the fuel cell. Due to the fuel cell's short lifespan and high price, it makes sense to apply a TCS to fuel cell electric tractors.

The TCS needs to set the upper and lower limits of the SOC. When the SOC is lower than the SOC lower limit (40%), the fuel cell starts (part of the fuel cell output power is delivered to the motor, and the rest is charged to the battery pack). When the SOC is above the SOC upper limit (80%), the fuel cell stops (the battery separately delivers electrical energy to the motor).

To realize the function of thermostat control strategy, four states are defined in this paper, which corresponds to the four operating states of fuel cell electric tractors.

State 1: The hydrogen is sufficient (the mass of hydrogen consumption M_{hyd} is less than 960 g), and battery SOC > 80. The battery alone supplies power to the tractor.

State 2: The hydrogen is sufficient, and battery 80 $\geq$ SOC > 40; fuel cell and battery output power according to Section 3.2.

State 3: The hydrogen is sufficient, and battery SOC $\leq$ 40; the fuel cell outputs the maximum constant current in the high-efficiency area, it meets the needs of the tractor operation, and the excess power is used to charge the battery.

State 4: The hydrogen is exhausted, and the fuel cell is shut down. The battery alone supplies power to the tractor until SOC $\leq$ 40.

The flow of the finite state machine and the transition conditions between states are shown in Figure 4.

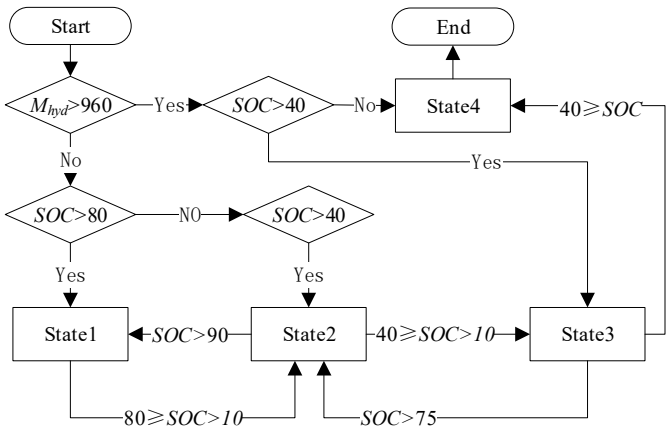

Figure 4. State flow.

3.2. EMS Based on PF

Although the TCS can maintain the SOC within a reasonable range, it will cause the fuel cell to start and stop frequently. When the SOC is high, the fuel cell output power is expected to be small, and when the SOC is low, the fuel cell output power is expected to be high. The output power of the fuel cell should follow the change of the battery SOC, and the power following (PF) strategy can well meet this requirement.

PF is practical and is widely used in the EMS of fuel cell vehicles. The control method for the fuel cell output power is based on the demand power and adjusted by taking the *SOC* value as the independent variable. Equations (8) and (9) give the solutions of fuel cell and battery output power in Section 3.1 (state 2).

$$P_{fc} = \lambda\left(\frac{SOC_{max} - SOC}{SOC_{max} - SOC_{min}}\right) \cdot \frac{P_{dem}}{P_{mot_max}} \cdot P_{fcmax} \tag{8}$$

$$P_{bat} = P_{dem} - P_{fc}\eta_{dc} \tag{9}$$

where P_{dem} is the demand power of motor, P_{mot_max} is the maximum motor power in the maximum efficiency range of the motor, η_{dc} is the efficiency of DC/DC converter, and λ is the adjustment coefficient.

3.3. Power Constraint Based on Fuzzy Logic Control

Sections 3.1 and 3.2 solve the problem of fuel cell output power. However, it does not restrict the dynamic output characteristics of the fuel cell. The maximum power change rate of the commercial fuel cell selected in this paper is limited to 300 W/s. When the demand power changes rapidly, the PF strategy requires the output power of the fuel cell to follow the demand power. Therefore, the output power change rate of the fuel cell will exceed 300 W/s, so the fuel cell power change rate needs to be restricted.

The output power of the fuel cell in the last second is recorded and saved as P_{fcl}, the target output power of the fuel cell (P_{fc_tag}) is calculated through PF, and the difference

between P_{fcl} and P_{fc_tag} is calculated as ΔP_{fc}. If $\Delta P_{fc} \leq 300$ W/s, the fuel cell output power is $P_{fc} = P_{fc_tag}$. If $\Delta P_{fc} > 300$ W/s, the fuel cell output power is $P_{fc} = P_{fcl} + \Delta P_{fc_real}$, the calculation of ΔP_{fc_real} is shown as follows.

In this paper, a fuzzy logic control (FLC) strategy is used to restrict the power change rate of fuel cells when $\Delta P_{fc} > 300$ W/s. FLC is an intelligent control method based on fuzzy sets, fuzzy language, and fuzzy reasoning. FLC has already been successfully applied in the field of powertrain and multi-energy distribution. In this study, a double-input single-output Mamdani fuzzy controller is designed based on FLC.

The fuzzy logic toolbox in MATLAB is used to design a fuzzy controller, the membership function of the FLC adopts the triangular membership function with better adaptability. The FLC has two inputs: one is the fuel cell power change rate (ΔP_{fc}). It should be noted that this power change rate is the difference between the target fuel cell output power calculated by the PF and the fuel cell output power in the last second. The range of ΔP_{fc} is [−600, 600], and four fuzzy subsets {NB, NS, PS, PB} are included. The second input of FLC is battery SOC. Since FLC only works in state 2, the fuel cell either has constant power or does not work in other states, so the SOC range is [40, 80], including five fuzzy subsets {PVS, PS, PM, PB, PVB}. The output of FLC is the increase of fuel cell output power (ΔP_{fc_real}), since the maximum power change rate of fuel cell is limited to 300 W/s. The output range of ΔP_{fc_real} is [0, 300], which includes five fuzzy subsets {NVB, NB, NM, NS, NVS}. Table 3 shows the specific fuzzy rules and Figure 5 shows the surface of FLC.

Table 3. Fuzzy ruler table.

ΔP_{fc_real}		ΔP_{fc}			
		NB	**NS**	**PS**	**PB**
SOC	PVS	VB	NVB	NVB	NB
	PS	NVB	NVB	NB	NM
	PM	NB	NB	NS	NM
	PB	NS	NM	NS	NS
	PVB	NVS	NVS	NVS	NVS

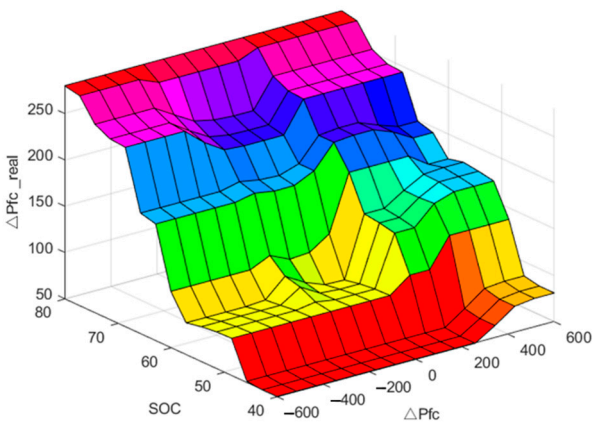

Figure 5. Surface of FLC.

3.4. Optimization Based on TS

FLC restricts the power change rate of fuel cell. However, the setting of fuzzy rules and weight coefficients are based on personal experience. The formulation of rules is subjective, and the control effect is not optimal. In this paper, a comprehensive energy consumption evaluation function is constructed considering energy consumption and fuel cell durability, which is shown in Equation (10).

$$Q = con_{hyd} \cdot C_{hyd}/s + Q_{max} \cdot C_{bat}/s + D_{fc} \cdot C_{fc}/(s \cdot 20) \tag{10}$$

where Q is the operating cost per mile, con_{hyd} is the total hydrogen consumption, s is the continuous operating mileage of the tractor, and 20 (%) is the maximum allowable percentage of fuel cell degradation in this paper. When the degradation of the fuel cell is more than 20%, the fuel cell will not continue to be used. C_{hyd}, C_{bat}, and C_{fc} are hydrogen price, electricity price, and fuel cell system price, respectively.

In this paper, Equation (10) is used as the global optimization function, and the tabu search (TS) algorithm is used for iterative optimization. The optimization objects are the membership function and weight coefficients of FLC. The optimization process is as follows: taking the endpoints and vertices of each membership function as the vector of the TS algorithm and recording them as (x_1, x_2, x_3, ... , x_{36}). Similarly, the weight coefficients of each fuzzy rule are also taken as the optimization objects of the TS algorithm and recording them as (y_1, y_2, y_3, ... , y_{25}). (x_1, x_2, x_3, ... , x_{36}) and (y_1, y_2, y_3, ... , y_{25}) satisfy the following constraints:

$$\begin{cases} \{x_1, x_2, x_3, \ldots x_{10}\} \in (-600, 600) \\ \{x_{11}, x_{12}, x_{13}, \ldots x_{23}\} \in (40, 80) \\ \{x_{24}, x_{25}, x_{26}, \ldots x_{36}\} \in (0, 300) \\ \{y_1, y_2, y_3, \ldots y_{25}\} \in (0, 1) \end{cases} \tag{11}$$

where (x_1, x_2, x_3, ... x_{10}) is endpoints and vertices of ΔP_{fc}'s membership function. (x_{11}, x_{12}, x_{13}, ... x_{23}) is endpoints and vertices of SOC's membership function. (x_{24}, x_{25}, x_{26}, ... x_{36}) is endpoints and vertices of ΔP_{fc_real}'s membership function. (y_1, y_2, y_3, ... y_{25}) is the weight coefficient of each fuzzy rule.

Figure 6 shows the locations of the vectors to be optimized for the membership function. The continuous ploughing mileage of the tractor is calculated through the simulation model, and the operating cost per unit mileage is calculated in Simulink based on the hydrogen consumption, fuel cell performance degradation, and battery power consumption. Finally, the membership function is continuously updated through MATLAB's m script file until the minimum operating cost is found. At this time, the corresponding membership function distribution and fuzzy rule weights are the final optimization results. Through offline optimization, the membership function and weight coefficients are no longer dependent on manual formulation, and the results are more objective. The flow of co-simulation with different algorithms is shown in Figure 7.

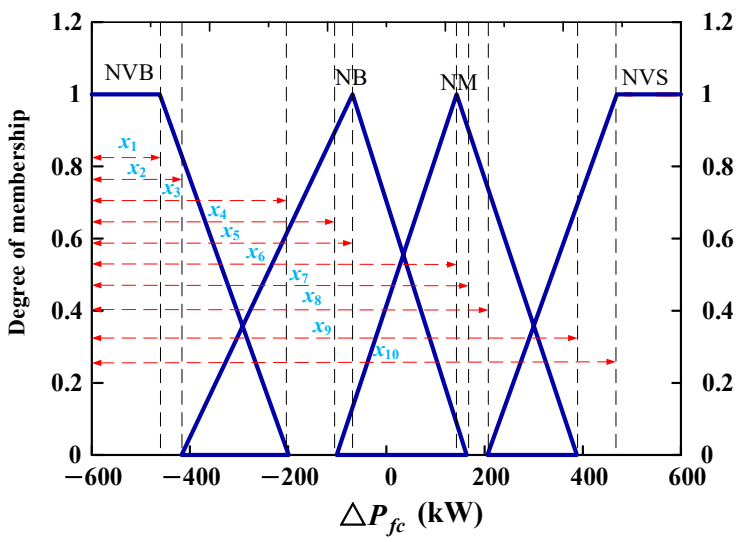

Figure 6. Vectors to be optimized for the membership function.

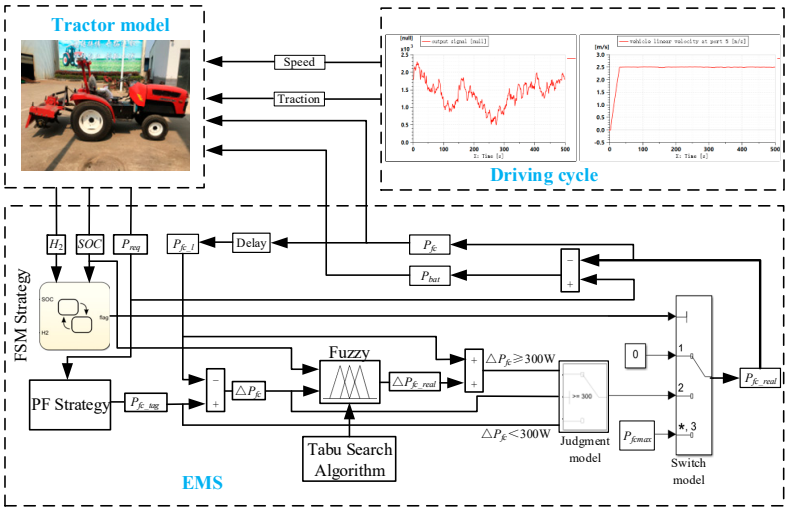

Figure 7. Co-simulation with different algorithms.

4. Results and Discussion

The ploughing resistance used in the simulation in this paper comes from the actual measurement in the field. The target ploughing speed of the tractor is 2.5 m/s, and the required power of the tractor calculated by simulation is shown in Figure 8. It can be seen from Figure 8 that the ploughing speed of the tractor can be maintained at the target speed of 2.5 m/s, and it can also be seen that the ploughing power of the tractor fluctuates wildly.

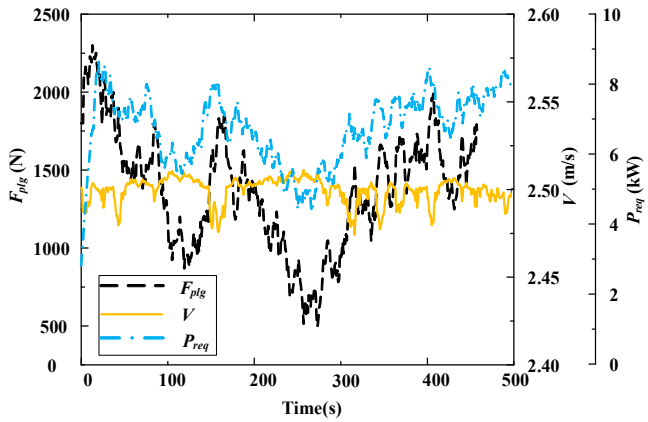

Figure 8. Ploughing traction force, simulated vehicle speed, and vehicle power demand.

After the optimization in Section 3.4, the membership function and weight coefficient of FLC are shown in Figure 9. Before the optimization, the distribution of the membership function is relatively regular. After the optimization, the distribution of the membership function becomes more random, but the control effect is better than that before the optimization. Figure 10 shows the comparison of fuel cell output power before and after optimization. When FLC is not optimized, the fuel cell output power fluctuates wildly. After optimization, the output power of the fuel cell becomes smoother, which is very beneficial to the service life of the fuel cell.

This paper further compares the control effects of EMS under different initial SOC states. Figure 11 shows that when the initial SOC (40%) of the battery is low, the fuel cell outputs the highest power in the high-efficiency region, the battery SOC begins to rise to 75% rapidly, the EMS enters state 2, the PF strategy controls the output power of the fuel cell. When the battery SOC is high, the fuel cell output power is small, and the battery output power is large. When the SOC is low, the output power of the fuel cell is large,

the power fluctuation is also significant, and the output power of the battery gradually decreases with the SOC.

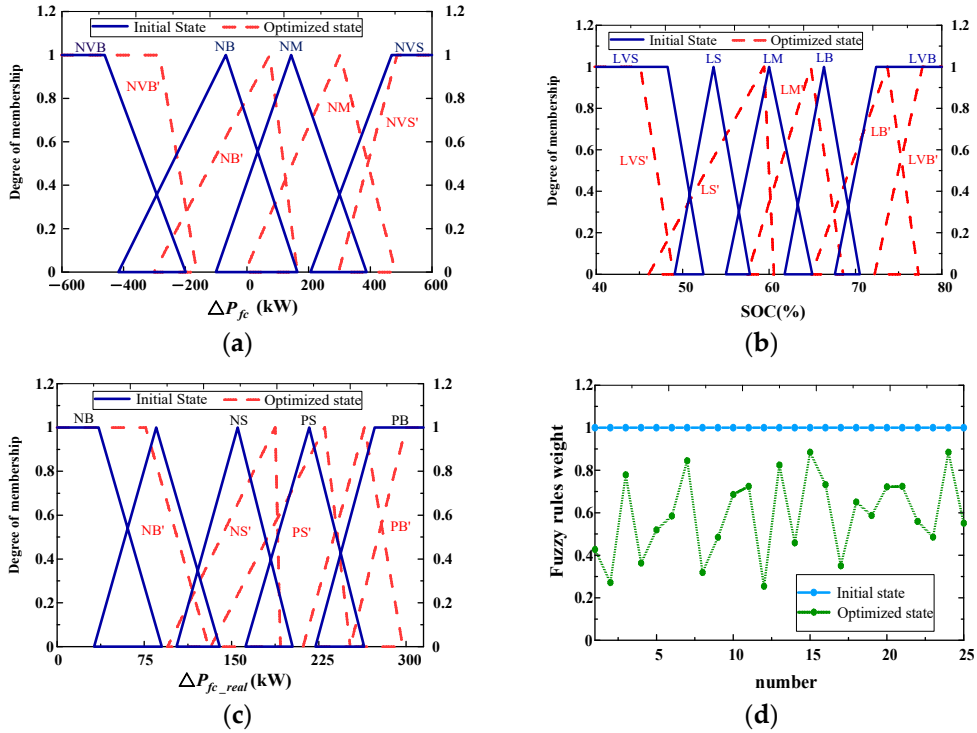

Figure 9. FLC membership function and weight coefficients before and after optimization; (**a**) membership function of ΔP_{fc}, (**b**) membership function of *SOC*, (**c**) membership function of ΔP_{fc_real}, (**d**) weight coefficients of FLC rulers.

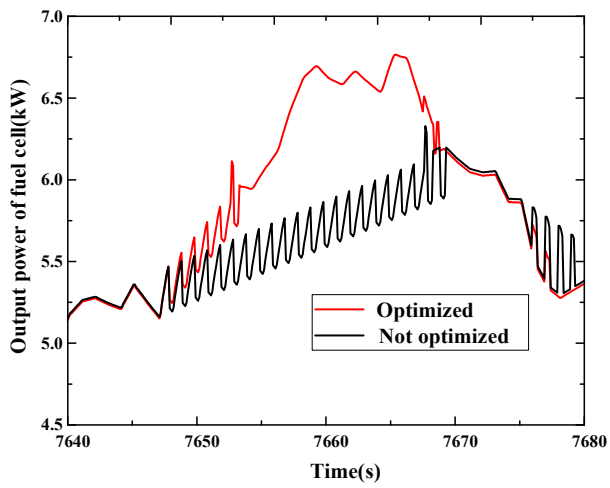

Figure 10. Comparison of fuel cell output power before and after optimization.

Figure 12 shows that when the initial SOC (65%) of the battery is middle. The EMS enters state 2, and the PF strategy controls the output power of the fuel cell. The SOC starts to decrease slowly until the SOC reaches 45%. Then the EMS enters state 3, and the fuel cell output power increases and remains constant. After the battery SOC rapidly rises to 75%, the EMS enters state 2 again. The fuel cell cooperates with the battery to supply power to the tractor until the SOC reaches 45%. The EMS enters state 3, the battery is charged, and the SOC rises. Finally, the hydrogen is consumed, and the battery alone provides electricity to the tractor until the SOC reaches 30%, and the tractor cannot continue to work.

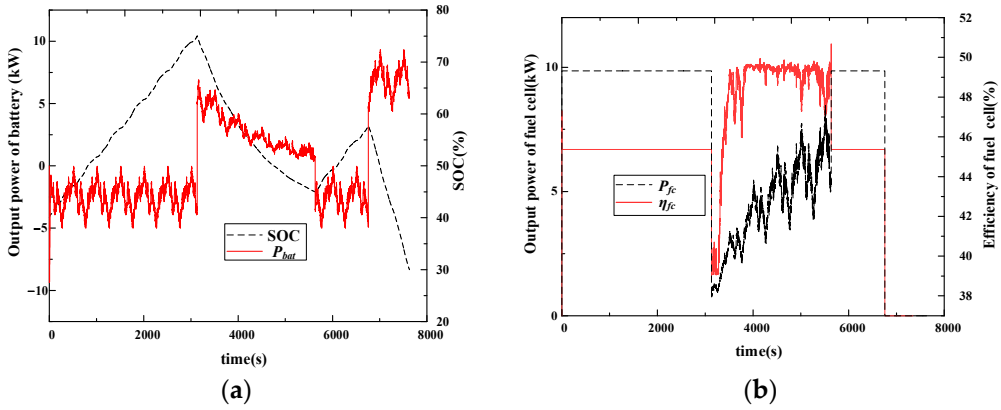

Figure 11. Performance of fuel cell and battery at an initial SOC of 40%. (**a**) Output power and SOC of battery, (**b**) output power and efficiency of fuel cell.

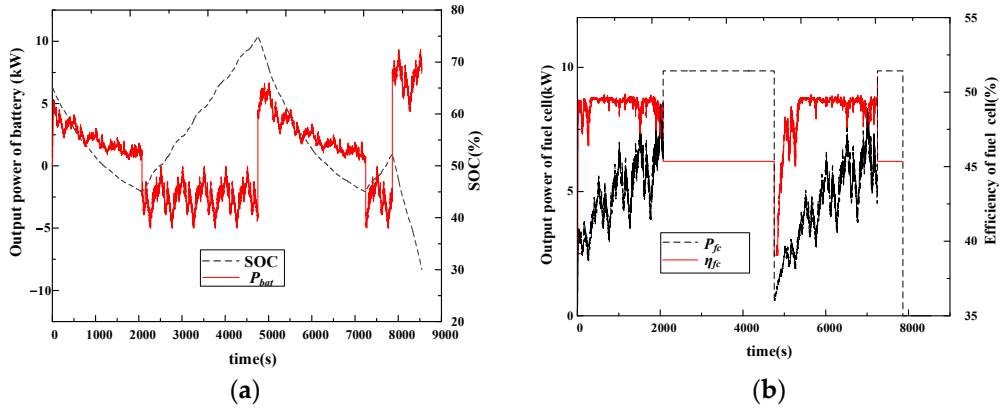

Figure 12. Performance of fuel cell and battery at an initial SOC of 65%. (**a**) Output power and SOC of battery, (**b**) output power and efficiency of fuel cell.

Figure 13 shows that when the initial SOC (90%) of the battery is high. The EMS enters state 1, and the battery alone provides electricity to the tractor. Then EMS enters state 2, and the SOC starts to decrease slowly until the SOC reaches 45%. The subsequent actions of the EMS are similar to Figure 12. It can be seen from Figures 11b, 12b and 13b that when the fuel cell switches from state to state, its power and efficiency fluctuate greatly. However, when the EMS is in state 2, the output power of the fuel cell is relatively stable, and the efficiency is also high.

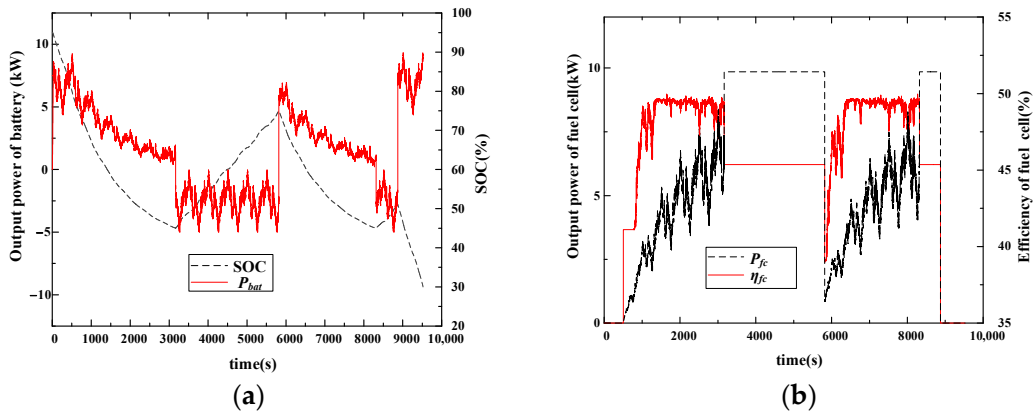

Figure 13. Performance of fuel cell and battery at an initial SOC of 90%. (**a**) Output power and SOC of battery, (**b**) output power and efficiency of fuel cell.

This paper further compares the performance of different EMSs on equivalent hydrogen consumption and fuel cell life degradation under 500 s ploughing conditions, as shown in Table 4. It can be seen from Table 4 that the proposed EMS has great advantages in protecting the service life of fuel cell, and the equivalent hydrogen consumption of the proposed EMS is also lower than that of FLC and PF. Since DP takes the lowest equivalent hydrogen consumption as the objective function, this algorithm can ensure the lowest equivalent hydrogen consumption. However, the protection of the fuel cell's lifespan is ignored, and the degradation of fuel cell is worse. It should be pointed out that the DP cannot be applied on real tractors because it relies on a known driving cycle.

Table 4. Performance comparison of different EMSs.

Strategies	Equivalent Hydrogen Consumption (g)	Degradation of Fuel Cell ($\times 10^{-4}$%)
Proposed strategy	58.72	1.572
FLC	59.63	2.931
PF	59.82	1.842
DP	57.33	1.632

5. Conclusions

In this paper, the fuel cell is applied to the tractor, and a new power system architecture is designed. The tractor equipped with this power system can break through the limitation of the operating mileage of the traditional pure electric tractor and has no pollution emission. An EMS based on multi-algorithm fusion and optimization is proposed. The output power of fuel cell and battery is reasonably distributed by PF strategy combined with current SOC. Secondly, the change rate of fuel cell power is constrained by fuzzy control. Finally, the membership function and weight coefficients of fuzzy control are optimized by TS optimization algorithm, which improves the economy of the system and the durability of the fuel cell. The proposed strategy can reduce the equivalent hydrogen consumption by 1.52 and 1.83% compared with FLC and PF, respectively, while reducing the lifetime decline by 46.3 and 14.7%, respectively. The proposed control strategy also provides help for the design of the tractor vehicle. At the same time, the proposed strategy has not yet minimized the equivalent hydrogen consumption. In the follow-up research, the thresholds for turning on and off the fuel cell need to be further optimized.

Author Contributions: Methodology, H.Y.; software, Y.S.; validation, H.Y., C.X. and H.Z.; writing—original draft preparation, H.Y.; writing—review and editing, Y.S.; visualization, C.X.; supervision, C.X.; project administration, C.X. All authors have read and agreed to the published version of the manuscript.

Funding: This work was supported by Science and Technology Support Program of Jiangsu Province. Project number: BE2018343-1. The authors would like to thank the National Key R&D Plan of China (NO. 2016YFD0700402) for the support given to this research. This work was also supported by the enterprise practice training project for young teachers in higher vocational colleges in Jiangsu Province (NO. 2021QYSJ005).

Conflicts of Interest: The authors declare no conflict of interest.

References

1. Vogt, H.H.; de Melo, R.R.; Daher, S.; Schmuelling, B.; Antunes, F.L.M.; dos Santos, P.A.; Albiero, D. Electric tractor system for family farming: Increased autonomy and economic feasibility for an energy transition. *J. Energy Storage* **2021**, *40*, 102744. [CrossRef]
2. Lombardi, G.V.; Berni, R. Renewable energy in agriculture, Farmers willingness-to-pay for a photovoltaic electric farm tractor. *J. Clean. Prod.* **2021**, *313*, 127520. [CrossRef]
3. Hammerl, J.; Schaub, H. Effects of Electric Potential Uncertainty on Electrostatic Tractor Relative Motion Control Equilibria. *J. Spacecr. Rocket.* **2022**, *59*, 552–562. [CrossRef]
4. Baek, S.Y.; Baek, S.M.; Jeon, H.H.; Kim, W.S.; Kim, Y.S.; Sim, T.Y.; Choi, K.H.; Hong, S.J.; Kim, H.; Kim, Y.J. Traction Performance Evaluation of the Electric All-Wheel-Drive Tractor. *Sensors* **2022**, *22*, 785. [CrossRef] [PubMed]

5. Nasathit, N.; Salim, M.A.B.; Photong, C. Design and Development of Electric Tractor using Simple Remote Control. *Eng. Access* **2022**, *8*, 112–122.
6. Liu, J.; Xia, C.; Jiang, D.; Sun, Y. Development and testing of the power transmission system of a crawler electric tractor for greenhouses. *Appl. Eng. Agric.* **2020**, *36*, 797–805. [CrossRef]
7. Xie, B.; Wang, S.; Wu, X.; Wen, C.; Zhang, S.; Zhao, X. Design and hardware-in-the-loop test of a coupled drive system for electric tractor. *Biosyst. Eng.* **2022**, *216*, 165–185. [CrossRef]
8. Beligoj, M.; Scolaro, E.; Alberti, L.; Renzi, M.; Mattetti, M. Feasibility Evaluation of Hybrid Electric Agricultural Tractors Based on Life Cycle Cost Analysis. *IEEE Access* **2022**, *10*, 28853–28867. [CrossRef]
9. Vaidya, A.S. A Study of Solar Electric Tractor for Small Scale Farming. *Int. J. Sci. Res. (IJSR)* **2019**, *8*, 1255–1259.
10. Ma, S.; Lin, M.; Lin, T.E.; Lan, T.; Liao, X.; Maréchal, F.; Van Herle, J.; Yang, Y.; Dong, C.; Wang, L. Fuel cell-battery hybrid systems for mobility and off-grid applications: A review. *Renew. Sustain. Energy Rev.* **2021**, *135*, 110119. [CrossRef]
11. Xie, R.; Ma, R.; Pu, S.; Xu, L.; Zhao, D.; Huangfu, Y. Prognostic for fuel cell based on particle filter and recurrent neural network fusion structure. *Energy AI* **2020**, *2*, 100017. [CrossRef]
12. Erixno, O.; Abd Rahim, N.; Ramadhani, F.; Adzman, N.N. Energy management of renewable energy-based combined heat and power systems: A review. *Sustain. Energy Technol. Assess.* **2022**, *51*, 101944. [CrossRef]
13. Sulaiman, N.; Hannan, M.A.; Mohamed, A.; Ker, P.; Majlan, E.; Daud, W.W. Optimization of energy management system for fuel-cell hybrid electric vehicles: Issues and recommendations. *Appl. Energy* **2018**, *228*, 2061–2079. [CrossRef]
14. Geng, C.; Jin, X.; Zhang, X. Simulation research on a novel control strategy for fuel cell extended-range vehicles. *Int. J. Hydrog. Energy* **2019**, *44*, 408–420. [CrossRef]
15. Miranda, M.H.R.; Silva, F.L.; Lourenço, M.A.M.; Eckert, J.J.; Silva, L.C. Electric vehicle powertrain and fuzzy controller optimization using a planar dynamics simulation based on a real-world driving cycle. *Energy* **2022**, *238*, 121979. [CrossRef]
16. Jin, F.; Wang, M.; Hu, C. A fuzzy logic based power management strategy for hybrid energy storage system in hybrid electric vehicles considering battery degradation. In Proceedings of the 2016 IEEE Transportation Electrification Conference and Expo (ITEC), Dearborn, MI, USA, 27–29 June 2016; IEEE: Piscataway, NJ, USA, 2016; pp. 1–7.
17. García-Triviño, P.; Llorens-Iborra, F.; García-Vázquez, C.A.; Gil-Mena, A.J.; Fernández-Ramírez, L.M.; Jurado, F. Long-term optimization based on PSO of a grid-connected renewable energy/battery/ hydrogen hybrid system. *Int. J. Hydrog. Energy* **2014**, *39*, 10805–10816. [CrossRef]
18. Mallon, K.R.; Assadian, F. Robustification through Minimax Dynamic Programing and Its Implication for Hybrid Vehicle Energy Management Strategies. *J. Dyn. Syst. Meas. Control* **2021**, *143*, 091001. [CrossRef]
19. Afrashi, K.; Bahmani-Firouzi, B.; Nafar, M. Multicarrier Energy System Management as Mixed Integer Linear Programming. *Iran. J. Sci. Technol. Trans. Electr. Eng.* **2021**, *45*, 619–631. [CrossRef]
20. Xu, N.; Kong, Y.; Yan, J.; Zhang, Y.; Sui, Y.; Ju, H.; Liu, H.; Xu, Z. Global optimization energy management for multi-energy source vehicles based on "Information layer-Physical layer-Energy layer-Dynamic programming" (IPE-DP). *Appl. Energy* **2022**, *312*, 118668. [CrossRef]
21. Huangfu, Y.; Li, P.; Pang, S.; Tian, C.; Quan, S.; Zhang, Y.; Wei, J. An Improved Energy Management Strategy for Fuel Cell Hybrid Vehicles Based on the Pontryagin's Minimum Principle. *IEEE Trans. Ind. Appl.* **2022**, *58*, 4086–4097. [CrossRef]
22. de Souza, E.A.G.; Nagano, M.S.; Rolim, G.A. Dynamic Programming algorithms and their applications in machine scheduling: A review. *Expert Syst. Appl.* **2022**, *190*, 116180. [CrossRef]
23. Yuan, H.B.; Zou, W.J.; Jung, S.; Kim, Y.-B. Optimized rule-based energy management for a polymer electrolyte membrane fuel cell/battery hybrid power system using a genetic algorithm. *Int. J. Hydrog. Energy* **2022**, *47*, 7932–7948. [CrossRef]
24. Lei, T.; Wang, Y.; Jin, X.; Min, Z.; Zhang, X.; Zhang, X. An Optimal Fuzzy Logic-Based Energy Management Strategy for a Fuel Cell/Battery Hybrid Power Unmanned Aerial Vehicle. *Aerospace* **2022**, *9*, 115. [CrossRef]
25. Ferahtia, S.; Rezk, H.; Djeroui, A.; Houari, A.; Fathy, A.; Abdelkareem, M.A.; Olabi, A. Optimal heuristic economic management strategy for microgrids based PEM fuel cells. *Int. J. Hydrog. Energy* **2022**, *in press*. [CrossRef]
26. Kamal, E.; Adouane, L. Optimized EMS and a Comparative Study of Hybrid Hydrogen Fuel Cell/Battery Vehicles. *Energies* **2022**, *15*, 738. [CrossRef]
27. Ruan, S.; Ma, Y.; Yang, N.; Xiang, C.; Li, X. Real-time energy-saving control for HEVs in car-following scenario with a double explicit MPC approach. *Energy* **2022**, *247*, 123265. [CrossRef]
28. Zheng, C.H.; Oh, C.E.; Park, Y.I.; Cha, S. Fuel economy evaluation of fuel cell hybrid vehicles based on equivalent fuel consumption. *Int. J. Hydrog. Energy* **2012**, *37*, 1790–1796. [CrossRef]
29. Ganesh, A.H.; Xu, B. A review of reinforcement learning based energy management systems for electrified powertrains: Progress, challenge, and potential solution. *Renew. Sustain. Energy Rev.* **2022**, *154*, 111833. [CrossRef]
30. Zhou, J.; Xue, Y.; Xu, D.; Li, C.; Zhao, W. Self-learning energy management strategy for hybrid electric vehicle via curiosity-inspired asynchronous deep reinforcement learning. *Energy* **2022**, *242*, 122548. [CrossRef]

31. Lagnelöv, O.; Larsson, G.; Nilsson, D.; Larsolle, A.; Hansson, P.-A. Performance comparison of charging systems for autonomous electric field tractors using dynamic simulation. *Biosyst. Eng.* **2020**, *194*, 121–137. [CrossRef]
32. Chen, Y.; Xie, B.; Du, Y.; Mao, E. Powertrain parameter matching and optimal design of dual-motor driven electric tractor. *Int. J. Agric. Biol. Eng.* **2019**, *12*, 33–41. [CrossRef]
33. Sun, Y.; Xia, C.; Yin, B.; Gao, H.; Han, J.; Liu, J. Energy management strategy for FCEV considering degradation of fuel cell. *Int. J. Green Energy* **2022**, 1–12. [CrossRef]
34. Song, K.; Chen, H.; Wen, P.; Zhang, T.; Zhang, B.; Zhang, T. A comprehensive evaluation framework to evaluate energy management strategies of fuel cell electric vehicles. *Electrochim. Acta* **2018**, *292*, 960–973. [CrossRef]